Positively Charged Surfactant-like Peptides Self-assemble into Nanostructures

Geoffrey von Maltzahn, Sylvain Vauthey, Steve Santoso, and Shuguang Zhang*

Center for Biomedical Engineering and Department of Biology, Massachusetts Institute of Technology, 77 Massachusetts Avenue, Cambridge, Massachusetts 02139-4307

Received September 9, 2002. In Final Form: January 14, 2003

A new type of surfactant peptide designed to mimic the properties of cationic lipid systems is described. These cationic surfactant peptides are approximately 2 nm in length with a cationic, hydrophilic head consisting of one to two residues of lysine or histidine followed by a hydrophobic tail of six alanine, valine, or leucine residues. In water, these surfactant peptides form ordered structures with dynamic behaviors. At pH below the pI values of the peptides, dynamic light scattering showed two distinct structural populations with average diameters of 50 nm (>95%) and 100−200 nm (<5%). Transmission electron microscopy visualization of quick-frozen samples revealed these populations to likely represent nanotubes and nanovesicles, respectively, showing great interplay between them. Above the pI, these structures are absent, having further self-assembled into large membranous sheets. These cationic surfactant peptides are distinct from other anionic surfactant peptides and have different applications, possibly being useful as carriers for encapsulation and delivery of a number of small water-insoluble molecules and large biological molecular systems, including negatively charged nucleic acids.

Introduction

The advancement of science, biotechnology, and medical technology generally requires the development of new biological materials.[1−6] While traditional methods of fabricating biomaterials through polymerizing organic compounds and processing polymers have had tremendous impact in medical science for a broad range of applications, including scaffolds for tissue regeneration[7,8] and controlled drug deliveries,[9−10] the continued discovery of new biomaterials requires new methods of creation. The introductions of molecular biology, recombinant DNA technology, and protein chemistry have provided alternatives to the traditional way of producing these materials. New materials based on biologically derived polymers, including peptides, lipids, and oligonucleotides, have been shown to exhibit properties beneficial to medical science[2−4,11−13] and will have significant implications in advances of future generations of materials.

We previously described our recent efforts in developing anionic surfactant peptides that undergo self-assembly to form well-ordered nanostructures.[14−15] These anionic peptides were molecular-designed and chemically synthesized to mimic the properties of polymeric and lipid surfactant molecules. One of the distinctive characteristics is that these surfactant peptides have a hydrophobic tail consisting of consecutive nonpolar amino acids, such as glycine, alanine, valine, leucine, or isoleucine, and a hydrophilic head consisting of the negatively charged amino acid aspartic acid or glutamic acid. The size of those surfactant peptides varies from 2.5 to 4.7 nm in length, corresponding to 7 to 12 amino acids.[14−15]

We are interested in further expanding the functional capabilities of self-assembling surfactant peptides by introducing several cationic surfactant peptide systems. These peptides are designed to mimic the surfactant properties of cationic lipid molecules, which are less readily amenable to modifications at the molecular level. This class of surfactant peptides has a headgroup consisting of one or two positively charged amino acids, such as lysine or histidine, and a tail of six hydrophobic amino acids. Molecular modeling showed that arginine's large guanidine group may interfere with the self-assembly process; thus, it was not used in the headgroups of the peptides in this study. Like lipids and anionic surfactant peptides, the cationic surfactant peptide molecules generally have a tendency to sequester their hydrophobic tails in aqueous solutions by self-assembling themselves into nanostructures. This self-assembly phenomenon is similar to the well-studied events in lipid, except that the nanostructures are several orders of magnitude smaller, as lipid surfactants generally form stable microstructures.[16−18]

These cationic surfactant peptides not only can be readily designed at the single amino acid level but also

* To whom correspondence should be addressed. Telepone: 617-258-7514. Fax: 617-258-0204. E-mail: shuguang@mit.edu.

(1) Peppas, N. A.; Langer, R. *Science* **1994**, *263*, 1715−1720.
(2) Yu, S. M.; Conticello, V. P.; Zhang, G.; Kayser, C.; Fournier, M. J.; Mason, T. L.; Tirrell, D. A. *Nature* **1997**, *389*, 167−170.
(3) Petka, W. A.; Harden, J. L.; McGrath, K. P.; Wirtz, D.; Tirrell, D. A. *Science* **1998**, *281*, 389−392.
(4) Nowak, A. P.; Breedveld, V.; Pakstis, L.; Ozbas, B.; Pine, D. J.; Pochan, D.; Deming, T. J. *Nature* **2002**, *417*, 424−428.
(5) Fields, G. B.; Lauer, J. L.; Dori, Y.; Forns, P.; Yu, Y. C.; Tirrell, M. *Biopolymers* **1998**, *47*, 143−151.
(6) Caplan, M. R.; Schwartzfarb, E. M.; Zhang, S.; Kamm, R. D.; Lauffenburger, D. A. *Biomaterials* **2002**, *23*, 219−227.
(7) Langer, R. *Mol. Ther.* **2000**, *1*, 12−15.
(8) Halstenberg, S.; Panitch, A.; Rizzi, S.; Hall, H.; Hubbell, J. A. *Biomacromolecules* **2002**, *3*, 710−723.
(9) Putnam, D.; Gentry, C. A.; Pack, D. W.; Langer, R. *Proc. Natl. Acad. Sci. U.S.A.* **2001**, *98*, 1200−1205.
(10) Lendlein, A.; Langer, R. *Science* **2002**, *296*, 1673−1676.
(11) Zhang, S.; Holmes, T.; DiPersio, M.; Hynes, R. O.; Su, X.; Rich, A. *Biomaterials* **1995**, *16*, 1385−1391.
(12) Holmes, T.; Delacalle, S.; Su, X.; Rich, A.; Zhang, S. *Proc. Natl. Acad. Sci. U.S.A.* **2000**, *97*, 6728−6733.
(13) Kisiday, J.; Jin, M.; Kurz, B.; Hung, H.; Semino, C.; Zhang, S.; Grodzinsky, A. J. *Proc. Natl. Acad. Sci. U.S.A.* **2002**, *99*, 9996−1001.
(14) Vauthey, S.; Santoso, S.; Gong, H.; Watson, N.; Zhang, S. *Proc. Natl. Acad. Sci. U.S.A.* **2002**, *99*, 5355−5360.
(15) Santoso, S.; Hwang, W.; Hartman, H.; Zhang, S. *Nano Lett.* **2002**, *2*, 687−791.
(16) Israelachvili, J. N.; Mitchell, D. J.; Ninham, B. W. *J. Chem. Soc.* **1976**, *72*, 1525−1568.
(17) Spector, M. S.; Easwaran, K. R.; Jyothi, G.; Selinger, J. V.; Singh, A.; Schnur, J. M. *Proc. Natl. Acad. Sci. U.S.A.* **1996**, *93*, 12943−12946.
(18) Selinger, J. V.; MacKintosh, F. C.; Schnur, J. M. *Phys. Rev. E: Stat. Phys.* **1996**, *53*, 3804−3818.

10.1021/la026526+ CCC: $25.00
Published on Web 02/05/2003

are made through standard commercial peptide synthesis. Furthermore, they can be easily modified and tailored to interact with other surfactant molecules, sugars, and proteins. They represent a new type of nanomaterial with potential utilities for specific recognition, controlled drug delivery, encapsulation, and delivery of negatively charged nucleic acids into cells.

Materials and Methods

Peptide Designs, Synthesis, and Preparation. The rationale for peptide sequence design was to create a peptide monomer of approximately phospholipid size containing a hydrophilic head and a hydrophobic tail. Within this framework, the peptide sequences were then designed with a constant length hydrophobic tail and either one or two amino acids in the headgroup. The hydrophobicity of the tail was varied by using different amino acids. The hydrophilic moiety of the peptide is supplied by the headgroup, where the number of positive charges was varied. The various sizes of amino acid side chains also affect self-assembly. The peptides presented here (Figure 1) were selected from a wide range of positively charged sequences on the basis that they were readily soluble in pure water. Those peptides that were insoluble in water at all pH values have, at present, not been studied further.

These peptides have two orientations. The peptides V_6K_2, L_6K_2, A_6K, V_6H, and V_6K (Figure 1) were synthesized with a Rink amide resin that bears no charge as the headgroup's first amino acid, continuing toward the acetylated N-terminus of the nonpolar tail. These molecules contain one positive charge at the headgroup for every charged amino acid in the sequence. In the opposite arrangement, H_2V_6 and KV_6 (Figure 1), a Rink amide resin which bears no charge was used for the C-terminal amino acid of the hydrophobic tail with a free N-terminus at the headgroup. This arrangement allows a single lysine or histidine to bear two positive charges at the N-terminus, one from the side chain and one from the N-terminus.

All the peptides were commercially synthesized by SynPep, Dublin, CA (www.synpep.com). These peptides were solubilized in sterile water at a concentration of 1 mg/mL (1−2 mM) in small scintillation glass vials and sterile filtered through a 0.2 μm filter. The solutions were then titrated to pH 4, pH 7, pH 9, or pH 12 (±0.02) using HCl or NaOH and sonicated for 5 min using a sonicating water bath (Aquasonic Model 50HT from VWR Scientific). The peptide solutions were stored for 2 days at room temperature before dynamic light scattering measurements were carried out.

Dynamic Light Scattering (DLS). Dynamic light scattering experiments were performed with PDDLS/Batch (Precision Detectors, Franklin, MA) on 200 μL aliquots of the 1 mg/mL peptide solutions. The Precision Deconvolve program was used for the measurement of average diameter and plotted the information as fractional distribution versus size. Each measurement was consecutively repeated five times, and consistent results were obtained. DLS is capable of detecting the presence of nanostructures in solution but does not distinguish the molecular organization and structure.

Quick-Freeze/Deep-Etch Sample Preparation for Transmission Electron Microscopy (TEM). Quick-freeze/deep-etch sample preparation for TEM followed the protocol described by Magid.[19] Aliquots (1−2 μL) of the peptides in water were placed on 3-mm gold specimen carriers and frozen rapidly in liquid propane (−180 to −190 °C) by using the TFD 010 plunge-freeze and transfer device (BALTEC, Balzers, Principality of Liechtenstein). The quick-frozen samples were stored in liquid nitrogen and transferred onto a cold stage (−180 °C) in the CFE-60 freeze−fracture system (Cressington Scientific Instruments, Cranberry, PA). The sample holder was then slowly warmed to −100 °C, and the sample surface was etched for 30 min by placing a cooled knife (−180 °C) directly above the samples. After etching, the specimens were rotary-shadowed with a 20° platinum−carbon gun. The estimated electron-dense coating thickness using this method was ∼1.5−2.0 nm, as determined by a quartz crystal thin-film monitor. Replicas were strengthened by evaporation of

(19) Magid, L. J. *J. Phys. Chem. B* **1998**, *102*, 4064−74.

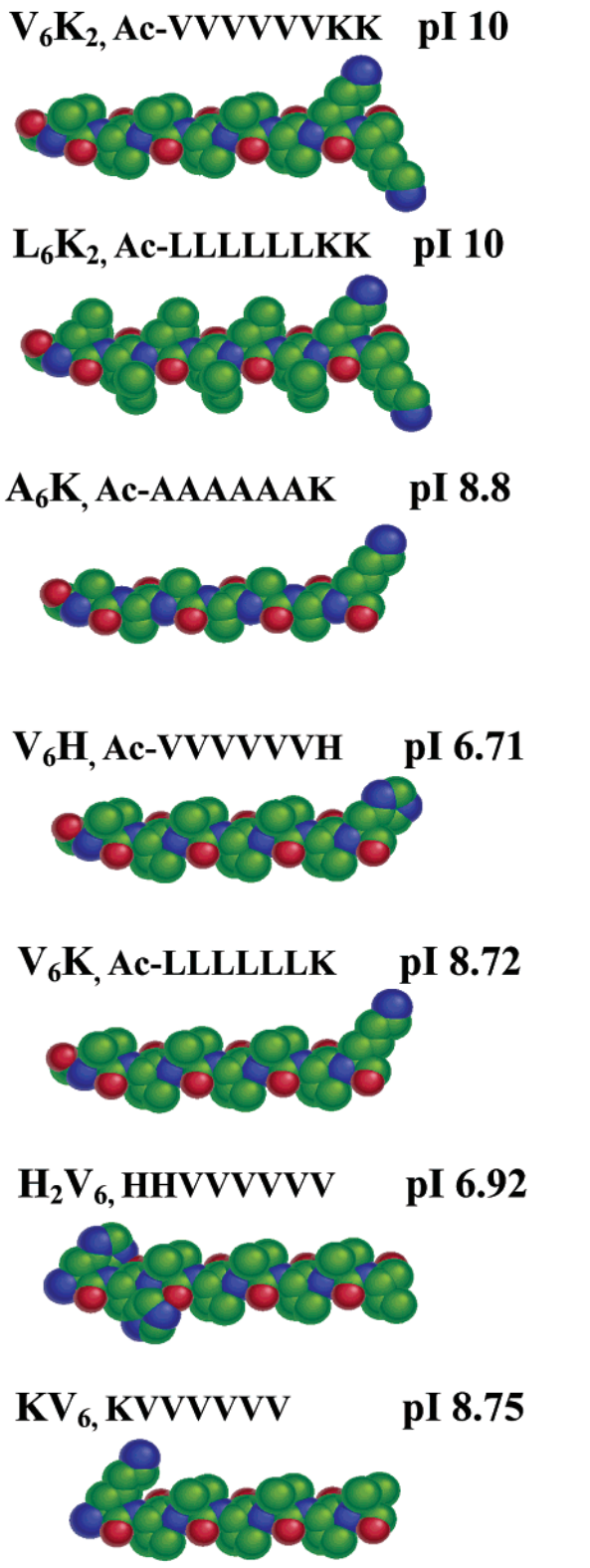

Figure 1. Molecular models of the peptides; N→C orientations. The subscript numbers represent the number of that amino acid appearing consecutively in the sequence. The peptides were synthesized in two orientations: with the headgroup at the C-terminus (the top five peptides) and with the headgroup at the N-terminus (the last two). The peptides are all approximately 2−3 nm in length and are geometrically larger at the heads. The color scheme is as follows: carbon, green; nitrogen, blue; oxygen, red. The theoretical pI values for the peptides are calculated according to the peptide sequence from the widely used website (http://www.expasy.ch/tools/pi_tool.html). These theoretical pI values are for the peptide monomers in solution, not for the assembled nanostructures.

carbon at an angle of 90°. The thickness of the carbon surface was ~15−20 nm. After shadowing, the sample with the replica coating was stored in methanol overnight and then treated with bleach to degrade the peptides. The remaining replicas were washed several times in distilled water and floated onto copper Gilder grids (Electron Microscopy Sciences, Fort Washington, PA). The replicas were then examined using a JEOL 200CX transmission electron microscope.

Results and Discussion

The cationic surfactant peptide sequences were designed to mimic amphiphilic lipid molecules of approximately 2−3 nm with a hydrophilic head and hydrophobic tail. We used one or two positively charged lysine or histidine groups as the headgroup to increase the solubility when more hydrophobic leucine residues were used. Furthermore, when two lysines are used, it also increased the peptide pI values to 10 instead of pI about 8.8 in the single lysine samples. We also placed the positively charged headgroups at either end of the peptides. Although having the C-terminus at the headgroup was preferential for solubility, no significant structural differences were observed in the present study, suggesting surfactant property does not depend on the orientation.

It is well-known that lipids, fatty acids, and organic and polymeric surfactant molecules spontaneously self-assemble in aqueous solution to form supramolecular structures in an entropy-driven process of eliminating the hydrophobic interactions between the hydrophobic tails and water.[16−18] This process is ubiquitous in nature, as it is the hydrophobic interactions that drive the self-assembly and afford the stability of many organized cellular structures including micelles, cellular organelles, membranes, the DNA double helix, and folded proteins.[16,20]

Dynamic Light Scattering (DLS). DLS is a powerful tool that can rapidly screen a large number of soluble samples for their innate ability to form structure in solution. We therefore first used DLS to estimate the average sizes associated with our self-assembly as a function of pH. DLS results were recorded for each peptide at pH 4, pH 7, pH 9, and pH 12 (±0.02). Two general trends were observed in the cationic surfactant peptides studied here.

First, below a peptide's pI, discrete nanostructures appear in solution. These nanostructures exist as two distinct populations in the DLS results; a predominant peak centered around 30−50 nm, and a much smaller one at about 100 nm (Figure 2A). These DLS results are essentially impervious to the pH changes below the transition point of the peptide. Second, above the pI of the peptide, the structures change dramatically and DLS can no longer accurately measure the size of structures in the peptide solutions (Figure 2B).

Figure 2 compares DLS data for V_6K_2 at pH 4 (Figure 2A) and pH 12 (Figure 2B) with the average autocorrelation functions in the insets. DSL records the light scattered by the sample across wavelengths for each time-point (t). The autocorrelation function is then calculated as an average measurement of the scattering function's similarity at two times, t_0 (a base signal) and $t_0 + \tau$ (a signal at some later time), in the experiment's time scale. The functions should ideally exhibit an exponential decay (as in Figure 2A) and provide the diffusion coefficient and thus the hydrodynamic radius of the system using Einstein's diffusion equation.[21] This hydrodynamic radius does not correspond to an actual structural radius (i.e. the radius of the nanotubes or vesicles) because the complex self-assemblies studied here do not obey Einstein's equation for diffusion of discreet spherical molecules. DLS is used only as a means of confirming the presence of structures and investigating the relative size distributions of structures in solution.

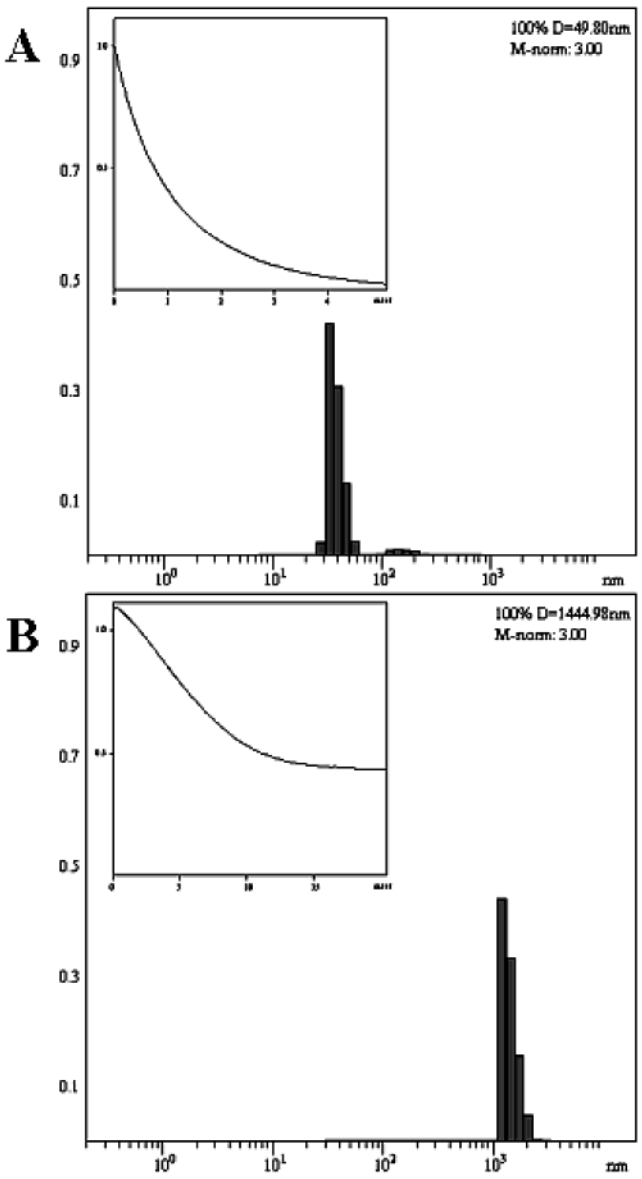

Figure 2. Dynamic light scattering (DLS) of cationic surfactant peptides (A) for the peptide V_6K_2 at pH 7 with the correlation function inset. Two populations of structures can be seen: one centered around 30−50 nm and the other centered on 100−200 nm. (B) Fractional population vs structural size for the same peptide at pH 12, above the pI of the system. Again the correlation function is inset, and we see it is now dramatically different, never reaching zero, as the structures are no longer on the nanoscale. The correlation functions should quickly approach zero for small dynamic assemblies such as those observed in our systems at low pH.

For pH well below the pI of the systems, we see the exponential decay of Figure 2A, whereas above the pI of the surfactant peptide the function never completely reaches zero (Figure 2B), regardless of the time scale used, making the fitting algorithm's size determination meaningless. Therefore, because there is some correlation between the signals throughout the experiment's time

(20) Edelhoch, H. Protein−lipid interactions and the role of water. *Horiz. Biochem. Biophys.* **1978**, *5*, 241−280.

(21) Magid, L. In *Dynamic light scattering: The Method and Some Applications*; Brown, W., Ed.; Oxford University Press: Oxford, 1993.

scale, the structures are too large for accurate measurement using our instrument (>1000 nm).

At these pH values above the transition point, the headgroups are effectively deprotonated, eliminating the electrostatic repulsion of the headgroups and causing the discrete nanostructures observed below their pI to flatten out into amorphous structures such as the membranous sheets observed using TEM in this study. When this critical transition event occurs, the solutions become cloudy and precipitate, as the structures are now large enough to scatter visible light.

This transition occurred for almost all cationic surfactant peptides once the pH was increased beyond the theoretical pI of the system: pH 9 for A_6K, V_6K, and KV_6; pH 7 for H_2V_6 and V_6H. The peptides V_6K_2 and L_6K_2 were exceptions, changing at pH 9, before their theoretical pI values. It should be noted that the theoretical pI values presented in Figure 1 only indicate the pI of the individual peptide molecules when completely solubilized in water and do not reflect the actual pI values of the self-assembled molecular structures. This lowered transition is, therefore, not surprising because the pI value for self-assembled systems can change by several pH units depending on the molecular architecture of the surfactant system (T. Zemb, personal communication).

TEM Examination of Samples Prepared through the Quick-Freeze/Deep-Etch Procedure. The quick-freeze/deep-etch preparation allows for visualization of the structures occurring in solution as the samples are quickly frozen in liquid propane (−180 to −190 °C), preventing ice crystal formation. The TEM images show a variety of structures within these systems, with great similarity across the different peptide sequences and orientations. All the sequences exhibited similar morphologies, with some form of the basic structures of nanotubes and vesicles. The two populations of nanotubes and vesicles likely represent the two peaks seen in DLS, as the nanotubes are generally smaller in diameter than the vesicles (approximately 30−50 nm vs approximately 100 nm) and much more prominent in solution. The preference in both the DLS (Figure 2) and the cryo-TEM (Figure 3) of V_6K_2 for the nanotube structures is observed across these systems. This consistent observation, using two different techniques, suggests the unambiguous existence of these ordered nanostructures.

Parallel arrays of nanotubes were observed in these peptide systems (Figures 3 and 4D), primarily within the three most defined DLS groups (V_6K_2, L_6K_2, and H_2V_6), with noticeable three-way junctions. Three-way junctions in nano- and microtubule structures have been implicated to be important in connecting the tubular structures and increasing the viscoelastic property of organogels.[22−23] Figure 3 shows the great complexity of these self-assembled structures at low magnification, where the monomers have created a supramolecular organization of branching, parallel structures spanning many micrometers. This image is indicative of all the systems below their pI's, as they all show a marked preference for the nanotube formations.

The TEM images also show that these systems are dynamic, with interplay between the populations of nanostructures at increased magnification. The high-resolution TEM images provide several examples of the structural diversity in the systems: for example, a region in A_6K where a nanotube may form segmented structures (Figure 4A), like a tubular balloon with divided segments;

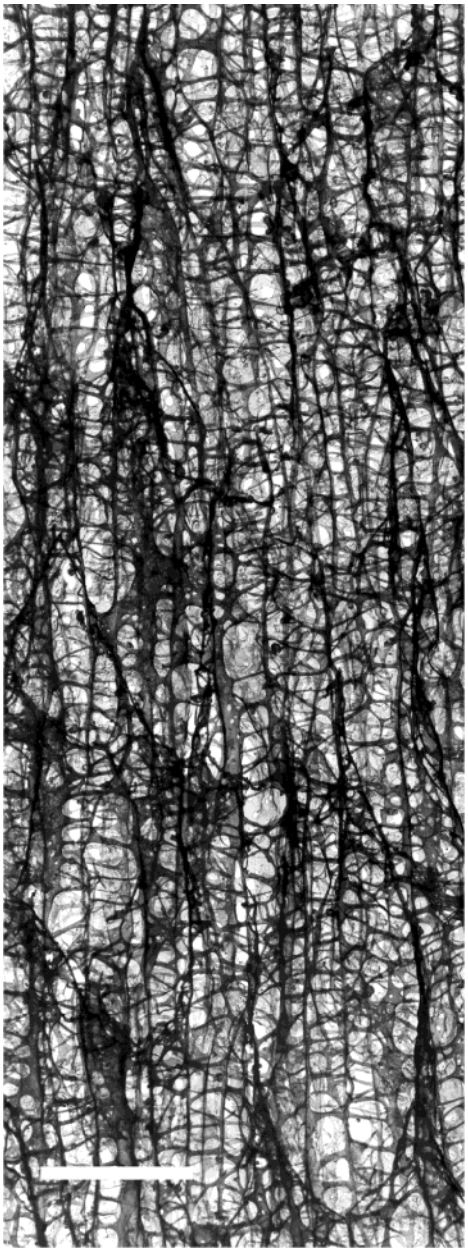

Figure 3. Quick-freeze/deep-etch TEM image of V_6K_2 in aqueous solution at pH 4 showing the great supramolecular organization of the nanotubes, spanning several micrometers. The tubes are interconnected through three-way and multiway junctions. The apparent density of the picture belies the nature of the system because we are seeing a 2-D picture of a 3-D network. A similar effect is felt if an aerial picture is taken of a tree without leaves. The scale bar represents 500 nm.

weblike images of H_2V_6 and V_6K_2 (Figure 4B and C, respectively); a region of nanotube arrays from L_6K_2 (Figure 4D); and vesicles from V_6K_2 (Figure 4E). The tubular balloonlike structure in Figure 4A is undergoing peristaltic or squeezing forces, resulting in a variance of the cross-sectional area about the center axis.[24] In some cases, lipid surfactant tapes may twist to produce similar images.[25,26] However, these twisted surfactant lipid structures usually have a much sharper appearance at the fold and appear, as they should, flat, much like a twisted party

(22) Cates, M. E. *Macromolecules* **1987**, *20*, 2289−2296.
(23) Cates, M. E. *J. Phys.* **1988**, *49*, 1593−1600.
(24) Israelachvilli, J. N. *Intermolecular and Surface Forces*; Academic Press: New York, 1992; pp 306−310.
(25) Svenson, S.; Messersmith, P. B. *Langmuir* **1999**, *15*, 4464−4471.
(26) Oda, R.; Huc, I.; Schmutz, M.; Candau, S. J.; MacIntosh, F. C. *Nature* **1999**, 299, 566−569.

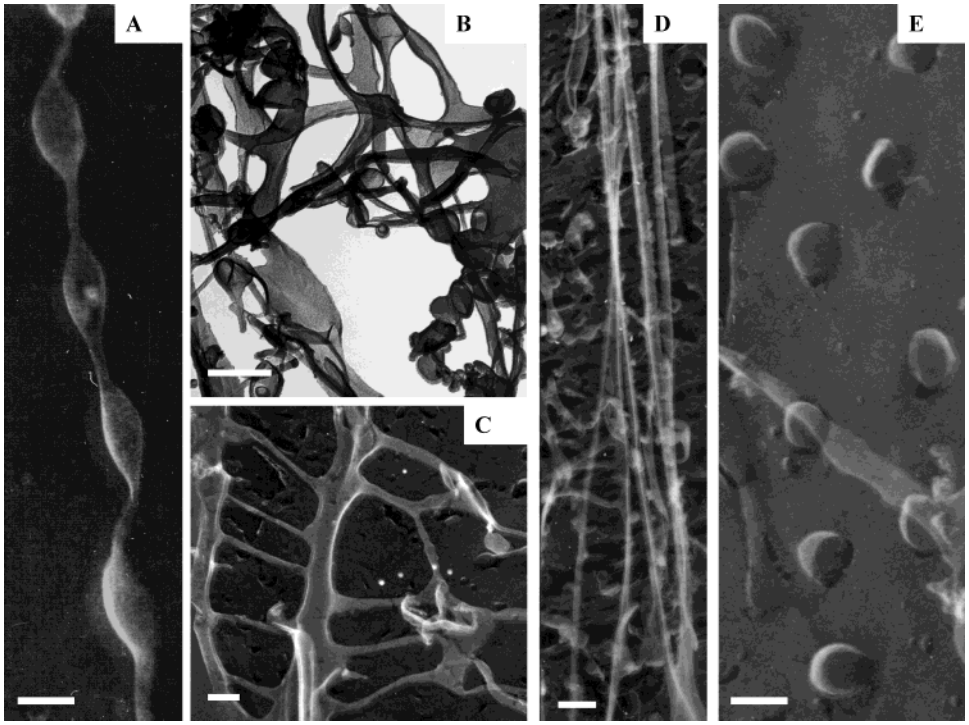

Figure 4. Quick-freeze/deep-etch TEM images illustrating the diversity and dynamic nature of cationic surfactant-like peptides: (A) A_6K pH 4; (B) H_2V_6 pH 4; (C) V_6K_2 pH 7; (D) L_6K_2 pH 7; (E) V_6K_2 pH 4. The structures beyond their pI values are not presented here because there are no obvious, well-defined nanostructures except membranous structures. Each scale bar represents 100 nm.

streamer, whereas the image in Figure 4A shows a smooth curvature associated with tubulelike structures. The cationic surfactant-like peptides do show some regions of flat, membranelike patches (lower left of Figure 4B) at low pH, but these membraneous patches do not show any periodic twist or pitch and appear instead either as flat areas or as what appear to be nanotubes that have been sliced open along one side.

The TEM images at pH values above the pI of the headgroups (data not shown) supported the idea that the nanotubes collapse and expand into membranous sheets, as the images, once rich with nanostructure, show instead vast flat expanses.

The dynamic nature of these systems and the structural similarity between peptide sequences is not unique to the cationic surfactant peptide systems. These structures exhibit great similarity to anionic surfactant peptides such as V_6D_2, L_6D_2,[14] and G_ND_2 where N represents 4, 6, 8, or 10.[15] These observations suggest that formation of these structures is sequence-sensitive but not sequence-specific.

Structure of Nonsurfactant Amphiphilic Peptides. The similarity of structure in this study is a result of specific molecular design to create peptide surfactants, not an intrinsic characteristic of seven to eight residue peptides. Marini et al. characterized the eight-residue peptide, FKFEFKFE, designed to be amphiphilic with two faces, one hydrophilic and the other hydrophobic, not surfactant in nature.[27] This EFK8 peptide formed a dramatically different structure, left-handed double-helical nanofibers that were observed both by the quick-freeze/deep-etch method/TEM and AFM.[27] Their observations confirm that structures correlate with the properties of designed peptide sequences. It should be pointed out that most peptides with few amino acids do not form well-ordered structures. They are either very soluble in water or insoluble, precipitating into disordered aggregates. The challenge is to design short peptides with well-defined structures.

Molecular Modeling. The peptide nanostructures represented here are similar to previously published nanotube and nanovesicle systems,[14−15] but the positively charged hydrophilic heads of these peptides allow for nanostructure at low pH, instead of precipitation out of water. We therefore propose the molecular tubular and vesicle models of these positively charged surfactant peptides (Figure 5). The proposed models depict a cutaway representation showing the hollow interior. The detailed mechanism of self-assembly for these cationic surfactant peptides into such proposed structures is largely unknown. Extensive modeling and simulations in subsequent studies will be required to understand this process. Although full computational modeling is beyond our current capability, we propose a likely course of self-assembly for the nanostructures observed in our experiments.

The process of surfactant self-assembly is an entropy-driven process of energy minimization in which the individual monomers pack together to sequester their hydrophobic tails from water. The negatively charged peptide surfactants are believed to form bilayers.[14] It seems likely that the cationic peptide nanostructures may also form a curved peptide bilayer. Within this curved bilayer, the peptides stack so that their hydrophilic heads are exposed to the water with their hydrophobic tails packed within. These proposed bilayers are approximately 4 nm in thickness due to a 2 nm length of single peptides and, because of both the peptide shape and the electrostatic repulsion among the headgroups, curve to form both nanotubes and vesicles. The packing of surfactant monomers into supramolecular structures has been well-described by the packing parameter of Israelachvili *et al.* [P = volume/(molecular length × cross-sectional area of the polar headgroup)].[16] This packing parameter characterizes the type of supramolecular structures seen on the basis of the monomer properties. The diverse struc-

(27) Marini, D.; Hwang, W.; Lauffenburger, D. A.; Zhang, S.; Kamm, R. D. *Nano Lett.* **2002**, *2*, 295−299.

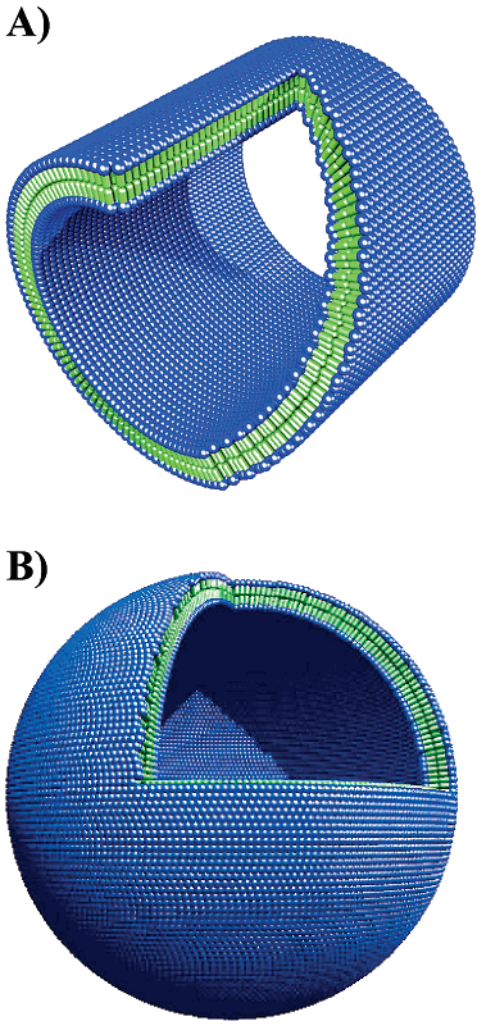

Figure 5. Proposed molecular models of cut-away structures formed from the cationic surfactant-like peptides at pH below their pI values. (A) Peptide nanotube with area sliced away. (B) Peptide nanovesicle. Color Code: blue, positively charged amino acid heads; green, hydrophobic tail. The peptides pack so that the polar heads are exposed to water, sequestering the hydrophobic tails within the bilayer, much like other organic polymer surfactants. The diameters of the nanostructures are about 50−100 nm.

tures observed here are likely due to the addition of the complex variables of hydrogen bonding between peptide backbones and electrostatic repulsion at the headgroups. As demonstrated by the pH variation above and below peptide pI's, the charge of the headgroups dramatically affects the structures seen. The nanovesicles and nanotube structures observed at pH values below the pI are modeled in Figure 5. Above the pI, these structures collapse to form membranous sheets.

Although the qualitative process of surfactant self-assembly is similar to that of lipid and fatty acid systems,[17,18] the peptide bilayer's internal chemistry is likely quite different due to the hydrogen bonds between peptide backbones and the increased rigidity of the peptide backbone.

Ghadiri and colleagues have reported another type of peptide nanotube where they used alternating D- and L-amino acids to form covalently linked rings which stack together to form tubular lattices.[28,29] They further show that these stacked rings can insert themselves into the cellular membrane.[30] Other investigators also reported design of peptide nanotubes, but in most cases, these nanotubes are lattice-forming structures.[31,32] The surfactant peptide nanotubes presented are much more dynamic, possessing the properties of traditional surfactants.

Lipid Surfactant Nano- and Microtubules. Schnur and colleagues have studied the nano- and microtubule formations of lipid surfactants for a number of years.[17,33] They used a variety of tools to characterize these well-formed structures. They reported that the lipid tubules form a left-handed helix with a defined pitch. They have also used metals to coat these nano- and microtubules for a number of applications.[34] These surfactant peptides in some ways mirror the lipid surfactant system but are almost an order of magnitude smaller in diameter.

Envisioned Applications. This new type of molecularly engineered surfactant peptides may have a broad range of applications, not only for areas where traditional surfactants are used, but also for growing biotechnology and emerging nanotechnology. Since the individual molecules can be designed and modified, they can be easily tailored for a variety of uses. These include encapsulation of water-insoluble molecules and delivery of biological molecules. Because these surfactants are made of amino acids that can be bioabsorbed and recycled, they may also be useful for cosmetic industries where other surfactants are used.

Furthermore, because these systems are positively charged, they can compact and encase negatively charged DNA and RNA for gene delivery. Currently, the area of gene therapy lacks DNA delivery systems that are efficient, nontoxic, nonimmunogenic, and simple to produce. Preliminary experiments using the cationic surfactant peptides presented here showed promise to compact DNA and to deliver DNA into several types of cells in cell culture.

Acknowledgment. We thank Dr. Wonmuk Hwang for molecular modeling of cationic surfactant peptide structures and Haiyan Gong of Boston University School of Medicine for helping with a TEM image. This work was supported primarily by the Engineering Research Centers Program of the National Science Foundation under NSF Award Number 9843342. We also acknowledge the Intel Corporation for providing us the educational high-performance computing facility.

LA026526+

(28) Ghadiri, M. R.; Granja, J. R.; Milligan, R. A.; McRee, D. E.; Khazanovich, N. *Nature* **1993**, *366*, 324.
(29) Fernandez-Lopez, S.; Kim, H. S.; Choi, E. C.; Delgado, M.; Granja, J. R.; Khasanov, A.; Kraehenbuehl, K.; Long, G.; Weinberger, D. A.; Wilcoxen, K. M.; Ghadiri, M. R. *Nature* (*London*) **2001**, *41*, 452−455.
(30) Ghadiri, M. R.; Granja, J. R.; Buehler, L. K. *Nature (London)* **1994**, *369*, 301−314.
(31) Gorbitz, C. H. *Chemistry* **2001**, *7*, 5153−5159.
(32) Ranganathan, D.; Samant, M. P.; Karle, I. L. *J. Am. Chem. Soc.* **2001**, *123*, 5619−5624.
(33) Schnur, J. *Science* **1993**, *262*, 1669−1676.
(34) Lvov, Y. M.; Spector, M.; Schnur, J. M. *Langmuir* **2000**, *16*, 5932−5937.